



DESIGN AND IMPLEMENTATION OF A TRANSISTORIZED BI-CONTROLLED BASED UTILITY-CONNECTED BATTERY CHARGER FOR UNDERDEVELOPED NATIONS

Z. Jagun¹, A. Okandeji^{2*}, C. Eya³, M. Olajide⁴, A. Ominike⁵, and S. Ukagu⁶

¹Department of Computer Engineering, Olabisi Onabanjo University, Ogun state, Nigeria

²Department of Electrical and Electronic Engineering, University of Lagos, Akoka, Lagos, Nigeria

³Department of Electrical Engineering, University of Nigeria, Nsukka, Enugu State, Nigeria

⁴Department of Electrical and Electronic Engineering, Olabisi Onabanjo University, Ogun state, Nigeria

⁵Department of Computer Science and Information Technology, Petroleum Training Institute, Effurun, Delta state, Nigeria

⁶Department of Electrical and Computer Engineering, Igbinedion University Okada, Edo State, Nigeria

*Corresponding author's email address: aokandeji@unilag.edu.ng

ARTICLE INFORMATION

Submitted 17 July, 2021
Revised 3 December, 2021
Accepted 10 December, 2021

Keywords:

Battery
Charger
Codeless
Nations
Underdeveloped

ABSTRACT

This paper presents a transistorized bi-controlled based utility-connected battery charger to address the problem of erratic public power supply in underdeveloped nations. In this study, a utility battery charger was built by the integration of grid power supply, line frequency transformer, power electronic switches, alternating current-direct current bridge converter, regulator, and resistor-inductor-capacitor. The excess-voltage protection and battery monitoring were obtained by the bi-controlled technique. In contrast to other charging systems in underdeveloped nations, the proposed system is very simple, rugged, reliable and cheap to maintain due to simplicity and un-programmed nature of the system. The results showed that the proposed system is craggy and robust to resist voltage stress, highly reliable and relatively free from leakage currents due to the presence of a double controlled scheme using a common point of action and a line frequency transformer. In addition, the system can be used to charge batteries ranging from 50 μ A and above. The system can be utilized in communication companies, electric vehicles, drilling machines.

© 2022 Faculty of Engineering, University of Maiduguri, Nigeria. All rights reserved.

1.0 Introduction

Communication and medical industries, navigating devices, transportable poly-media players, cable-less deployed remotes, and movable drilling machine needs rechargeable batteries to boost their working efficiencies (Tar and Fayed, 2016). Apart from the aforementioned fields of life, erratic public power supply in underdeveloped nations generally has forced these nations to utilize rechargeable batteries. The impression is to use the charged batteries to support the continuation of the services in those areas in the absence of grid power supply.

There are currently not less than 144 underdeveloped nations globally. The erratic power supply in these countries has triggered the use of rechargeable batteries. However, inappropriate charging and over-discharging of secondary batteries, especially in mechanical and electric workshops, are the main causes of battery damages (Esther et al., 2013). Additional cause of battery damage in underdeveloped nations is the inability to repair the micro-controller based battery chargers locally due to lack of innovative technical know-how. Essentially, underdeveloped nations repair faulty foreign battery chargers by replacing the faulty panel with a new panel. This increases the cost of maintenance, littering the environment, increasing the rate of pollution, and in extreme cases, poses health challenges to the public. The reason is that the majority of the

battery charger repairers in underdeveloped nations do not have the technical expertise about the coded integrated circuit parts in the damaged chargers. Secondly, instructions on panel repair are mostly hidden by the manufacturers. The secondary battery charging, on the other hand, needs good controllers to obtain a good state of charge (SOC) and a long-lasting life span of the battery (Woo *et al.*, 2011). Due to their broad working temperature array, stumpy self-discharge, extensive service life and maintenance free operations, lead acid batteries are commonly utilized. Secondary batteries can be charged either by renewable or non-renewable power sources. Renewable energy such as solar energy from the sun has the problem of decreasing the efficiency of charging batteries due to fluctuations in solar irradiations and varying environmental temperatures (Eya and Agu, 2015). Fossil fuel based charging source is a good option of the battery charging sources due to its relative constant supply, even though it has its own problems of environmental pollutions and oil spillage.

Utility battery charging systems (UBCS) can be unidirectional or bidirectional converters (Yilmaz and Krein, 2013., Hart, 2011). Under unidirectional condition, the UBCS make use of power diodes to rectify alternating current (AC) power to direct current (DC) power but utilizes IGBTs and MOSFETs under bidirectional process. Utility battery charging systems are often found in telecommunication industrial storage systems, ministry of transportations, electrical home inverter backup systems, hospital battery-based equipment (Agu, 2019).

There are various approaches in the charging system of a battery. These approaches include steady voltage (SV) or constant voltage (CV), constant current (CC), constant current constant voltage (CCCV), and pulse charging (Lee *et al.*, 2013, Tar and fayed, 2016). The easiest method is the steady voltage charging scheme (Lee *et al.*, 2013, Copea and Podrazhansky, 1999, Hua and Lin, 2000). The SV charging current depends on the voltage source. The charging current of the battery decreases once the voltage of the battery starts rising. In addition, the current might be excessively rated at the onset charging level if the battery is at a small capacity before charging. The CC method utilizes a steady current to charge the battery so that it can trim down the duration of charging efficiently (Hart, 2011). However, this could possibly lead to overcharging and hence, the temperature of the battery could rise rapidly after it is completely charged.

The mode of CCCV charging is realized by joining both CC and CV charging schemes (Hua and Lin, 2000, Hart, 2011, Chen and Lai, 2012). At the onset charging phase, the steady current is utilized to charge the battery until it gets to an excessively charged point or an initially defined voltage. This charging type then switches to CV phase to uphold the battery capacity. The merit is that the duration of charging could be drastically minimized. However, a more complicated regulatory circuit is needed, and a holding current could not be practically controlled efficiently. In pulse charging schemes, each charging cycle is engaged in “ON” and “OFF” per frequency for better charging effectiveness (Karami *et al.*, 2007, Dhar *et al.*, 2001, Chen, 2007, Eya *et al.*, 2019). However, the systems and their control techniques are complex, possess high power losses, advanced technical know-how, and high maintenance.

Meanwhile, considering the epileptic state of the economy of underdeveloped countries, low level of technical know-how, poor maintenance practice, intermittent lockdown due to the covid-19 pandemic, and the negative effects of the damaged rechargeable batteries in these nations as well as the complex controls of the aforementioned schemes, this study presents a codeless bi-controlled based utility-connected battery charger for underdeveloped nations. In particular, the objective of this study is to investigate the design of a power circuit and the codeless bi-controlled relay-based battery control scheme.

The proposed system possesses a simplified power charging circuit, uncomplicated control circuit, rugged isolated power transformer, transistorized circuit components, and a reliable over-voltage and excess charging protections. Therefore, the system can easily be implemented by a user once the circuit configurations are followed unlike other charger systems that are very complicated, coded with several hidden procedures for implementation. Furthermore, the proposed system is user friendly in terms of maintenance. Accordingly, even under seriously covid-19 pandemic lockdown, it can be locally repaired without removing the entire panel in case of any fault.

2. Materials and Methods

The method adopted in this study is the design-and-implementation scheme. Figure 1 consists of a power AC source, step-down transformer, H-bridge, uncontrolled AC-DC converter, filter and charger circuits. The charger circuit is sub-divided into LM317 section, and transistor-transistor coupled circuit. The LM317 part takes care of charging the battery of 12 V with current ranging from 50 μ A to 2.5A while transistor-transistor coupled circuit charges above 2.5A to 20.5A.

2.1. System Component Design

2.1.1. Transformer Design

The primary turns N_p of the transformer is derived as shown in (Kirchev et al., 2007)

$$N_1 = \frac{0.694V_p}{f\phi} = \frac{0.694V_p}{fBA}. \quad (1)$$

The electrical power in the primary side of the transformer is transferred to the secondary side due to magnetic coupling between them. Accordingly, f = frequency = 50Hz, B = Magnetic flux density and A = Cross-sectional area of the transformer.

The cross-section area of the transformer is given as (Kirchev et al., 2007)

$$A = L \times W, \quad (2)$$

where L = length, and W = width of the transformer. With the aid of the measuring rule, $l = 5.7cm = 0.057m$, and $w = 4.2cm = 0.042m$. Inserting the values of L and W in equation 2, the cross-section A becomes $2.394 \times 10^{-3}m^2$.

Given that $B = 1.210Wb/A$, supply voltage $V_p=230V$, and $f = 50Hz$, then equation 1 is used to compute the primary coil of the transformer to be 358 turns. The secondary coil number N_2 is obtained by using equation 3 as shown in (Kirchev et al., 2007).

$$N_s = N_p \times V_p^{-1} \times V_s \quad (3)$$

From equation 3, $N_2 = 28$ turn.

V_s = secondary voltage of the step-down transformer

2.1.2. Single Phase AC –DC Circuit Design

The DC output voltage and current of the H-bridge rectifier are expressed as shown in (Chen, 2009, Charles and Sadiku, 2009).

$$V_{dc} = 0.637 \times V_s \sqrt{2} \quad (4)$$

$$I_{dc} = \frac{2 \times I_s \sqrt{2}}{\pi} \quad (5)$$

16.2V and 21.6A are realized by inserting the secondary voltage of the transformer $V_s = 18V$ and secondary current $I_s = 24A$ into equation 4.

The power output of the AC–DC converter as given in (Charles and Sadiku, 2009) becomes

$$P_o = V_{dc}I_{dc} \quad (6)$$

P_o is computed by inserting 16.2V and 21.6A into equation 6 which yielded 349W. Under lossless conditions, the power output of the rectifier is equal to the power input to the charger section. Hence, the power of the charger can be approximated to be 349W.

2.1.3. LM 317 Design Circuit

The LM 317 section is regulated using equation 7 as in (Charles and Sadiku, 2009).

$$\frac{V_{dc}}{V_{ref}} - \frac{R_3}{R_4} = 1 \quad (7)$$

V_{ref} , R_3 and R_4 are reference voltage and resistances, respectively.

R_1 and R_2 are calculated using the expression in equation 8 and equation 9, respectively, (Charles and Sadiku, 2009).

$$R_1 = \frac{kV_{dc}}{I_{dc}} \quad (8)$$

$$R_2 = 5R_1, \quad (9)$$

where k is the constant ($0.7 \leq k \leq 0.74$)

2.1.4. Determination of Inductance, Resistance and Capacitance Design

The inductance of the inductor L_s is determined using the expression in equation 10.

$$L_s = \frac{V_{dc} - V_{R2} - V_{c2}}{\Delta I_L / \Delta t} \quad (10)$$

Where V_{c2} , V_{R2} , Δt and ΔI_L , respectively, represents the voltage across C_2 , voltage across R_2 , change in time duration, and current flowing through the inductor

The resistances of the resistors R_7 , R_8 and R_9 in Figure 2 are, respectively, expressed in equations 13, 14 and 15.

$$270k\Omega \leq R_5 \leq 300k\Omega \quad (11)$$

$$10k\Omega \leq R_6 \leq 20k\Omega \quad (12)$$

$$9.1k\Omega \leq R_7 \leq 10.2k\Omega \quad (13)$$

$$1k\Omega \leq R_8 \leq 2.2k\Omega \quad (14)$$

$$1.1k\Omega \leq R_9 \leq 2.2k\Omega \quad (15)$$

$$10.2k\Omega \leq R_{10} = R_{11} \leq 15.2k\Omega \quad (16)$$

$$3.1k\Omega \leq R_{12} \leq 4.2k\Omega \quad (17)$$

$$2.1k\Omega \leq R_{13} = R_{14} \leq 5k\Omega \quad (18)$$

$$5.1k\Omega \leq R_{15} = R_{16} \leq 10k\Omega \quad (19)$$

$$470\mu F \leq c_3 \leq 500\mu F \quad (20)$$

$$47\mu F \leq c_3 = c_4 \leq 50\mu F \quad (21)$$

The input and output capacitances of the capacitors C_1 and C_2 are related as shown in equation 22:

$$C_2 = \frac{C_1}{2}. \quad (22)$$

Where C_1 is in the range of $250\mu F \leq C_{1\leq} \leq 500\mu F$.

The proposed circuit diagram shown in Figure 1 is made up of di-charging modes, viz: R1-LM317-R3-R4 charging mode, and T1-R2-T2-T3-Ls charging mode. The dual charging modes do not supply the battery current simultaneously. If the current capacity to charge a battery is greater than what the R1-LM317-R3-R4 charging mode can carry out, it transfers the charging action to T1-R2-T2-T3-Ls charging mode to handle.

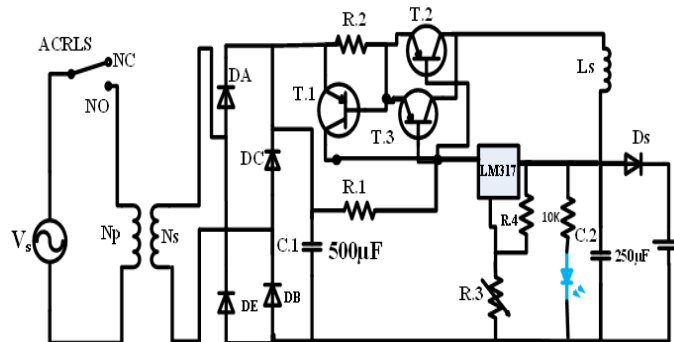


Figure 1: Proposed Circuit diagram

2.2 Working Principle of the Proposed System

An isolated 12V biasing voltage is supplied to V1, V2, V3, V4, V5 and V6 points as shown in Figure 2. Then, current flows from point V3 via R13 to the base terminal of transistor T5. The transistor T5 drives the current from V4 to the base terminal transistor T6 which spontaneously drives the current from point V5 to ground. This action drops zero voltage at the base terminal of transistor T4. Then, transistor T7 conducts current from V6 to close the relay switch at normally open (NO) point. As soon as the relay is put in the active condition (that connecting the source and load), the system starts charging the battery.

The charging of the battery connected to the proposed charger depends on the current drawn by the connected battery to the charging system. If the current drawn by the battery ranges from $50\mu A$ to 2.5A, the R1-LM317-R3-R4 charging mode circuit charges that battery but if the current required for charging the battery is more than 2.5A, the internal pass transistor of the LM317 dispels more energy than the allowable limit, and the LM317 charger section gets shut down. At this point, the LM317 regulator section is protected against overloads and short-circuits. Under the condition of the current being above 2.5A, the voltage-drop across R1 increases and transistors T2 and T3 bypasses the excess battery current LM317 cannot handle, and then the R1-LM317-R3-R4 charging mode takes over the charging process. The circuit components R2, T2 and T3 protect T1 from current above 2.5A and then charge the battery.

2.3 Transistorized Bi-Controlled Technique

The transistorized bi-controlled technique is shown in Figure 2. It consists of two arm sub-circuits joined together with aid of 4071B for controlling the over-voltage conditions in the system. One arm sub-circuit produces V_{so} . The V_{so} is activated to disconnect the AC relay (ACRLS) from the load line when the AC input voltage is more than 230Vrms. The second arm sub-circuit produces V_{Bo} . V_{Bo} is produced when the battery voltage is more than 14.40V. The second arm sub-circuit of Figure 2 shows the circuit diagram for charging and regulating over-charged state of the battery that is, having above 14.4V. As the battery continues to charge, the zener diode

Zd monitors the level of the battery voltage. Once the battery voltage is above 14.4V, Zd breaks down and acts as a resistive load. Then, current flows from the battery terminal and enters the base terminal of transistor T1. This scenario drives T4 to conduct current from point V3 through R13 to ground. Immediately, a zero voltage is placed at the base terminal of T5. Then, T5 and T6 stops conducting. Subsequently, 12V is placed at the base terminal of T7 through R14 and it blocks T7 from conducting. The resultant effect is that the Relay switch RLS disconnects and remains open, and the charging action stops. When the Zd recovers from the break down effect and the battery voltage becomes less than 14.4V, the charging process repeats itself. By so doing, the battery cannot be excessively charged.

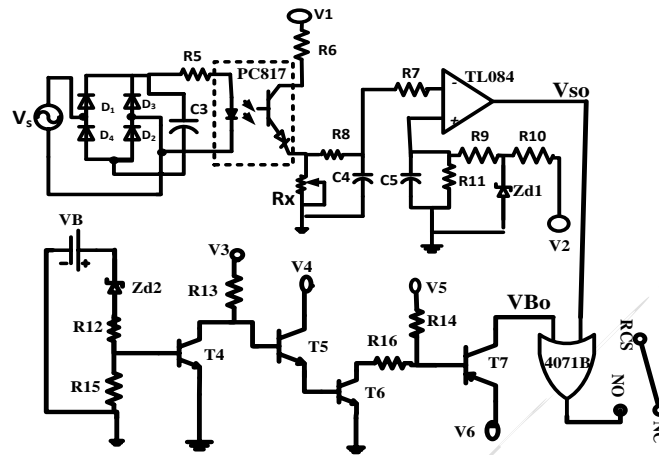


Figure 2: Codeless bi-controlled technique

3. Results and Discussion

The experimental set-up and results are shown in Figures 3-6. An un-energized set-up and zero voltage waveform on both analog oscilloscope and digital multimeter are shown in Figure 3. The battery, digital multi-meter, and oscilloscopic display is shown in Figure 3. It is observed that the level of the battery voltage, as displayed by the digital multi-meter, was 11.7VDC under active operation of the system as well as the commencement of battery charging.

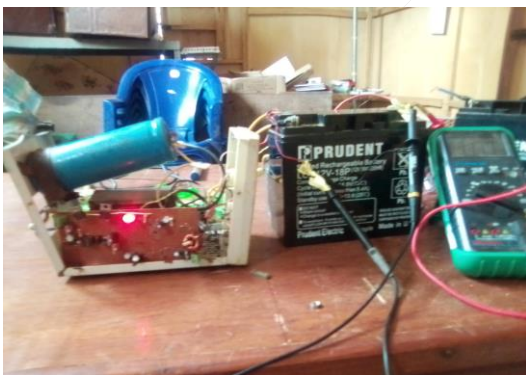


Figure 3: 11.7 VDC battery voltage from the digital meter with the proposed system



Figure 4: 12.23VDC battery voltage from digital meter with the proposed system

The progressive battery charging is shown from Figures 4 to 6. It is observed that Figure 4, 5 and 6 recorded 12.23V, 14.36V and 14.40V at time durations of 9:00am, 9:47am and 10:12pm, respectively. Finally, the charging of the battery stopped immediately the battery voltage reached 14.40V and that is exactly when there was zener diode break down which is shown in Figure 6.



Figure 5: 14.36VDC battery voltage from digital meter with the proposed system



Figure 6: 14.40VDC battery voltage from digital meter with the proposed system

Analytically, for the first forty minutes, as shown in Figures 4 and 5 the rate at which the battery was charged was very fast.

4. Conclusion

In this study, a transistorized bi-controlled based utility-connected battery charger for underdeveloped nations was investigated. The proposed system was designed, developed and validated with pictorial displays. The proposed system was observed to be fast with peak charging time of 1hr 12minutes being the time taken to fully charge the battery to 14.40V. The charging of the battery stopped immediately the battery voltage reached 14.40V and this is as a result of the zener diode break down. The charger has a capacity of 349W. The system can be utilized in electric vehicles, storage systems for telecommunication base stations, and home inverter system. A major disadvantage of the proposed system is its heavy weight, with relative power loss due to the line frequency transformer. Minimizing these drawbacks should be the focus of future research.

References

- Agu, MU. 2019. Principles of Power Electronics, Circuits. University of Nigeria Nsukka Press, Nsukka, Nigeria.
- Charles, KA., and Sadiku, MN. 2009. Fundamentals of Electric Circuits. McGraw-Hill Companies. Inc. 1221 Av. New York, 4th Edition.
- Chen, BY., and Lai, YS. 2012. New Digital-Controlled Technique for Battery Charger with Constant Current and Voltage Control without Current Feedback. IEEE Transactions on Industrial Electronics, 59(3):1545-1553.
- Chen, LR. 2007. A Design of an Optimal Battery Pulse Charge System by Frequency-Varied Technique. IEEE Transactions on Industrial Electronics, 54(1): 398-405.
- Copea, RC., and Podrazhansky, Y. 1999. The Art of Battery Charging. 14th Annual IEEE Battery Conference on Applications and Advances. 12-15, January. Long Beach, USA. pp. 233–235.
- Dhar, SK., Fetcenko, MA., and Ovshinsky, SR. 2001. Advanced Materials for Next Generation High Energy and Power Nickel-Metal Hydride Portable Batteries. 16th Annual Battery Conference on Applications and Advances, 1 January, California, USA., pp. 325- 336.

Esther, GS., Dhivya, PS., and Sivaprakasam, T. 2013. Solar Powered High Efficient Dual Buck Converter for Battery Charging. *International Journal of Innovative Research in Electrical Electronics Instrumentation and Control Engineering*, 1: 449-521.

Eya, CU., and Agu, MU. 2015. Solar based boost differential inverter. *Nigerian Journal of Technology (NIJOTECH)*, 31 (1): 164-167.

Eya, CU., Ejiogu, EC., Agu, MU., and Nnadi, DB. 2019. Transformer-less Voltage Stabilizer Controlled By Proportional Plus-Integral (PI) Controller. *MAT Journal of Power Electronics and Devices*, 5(3):42-51.

Hart, DW. 2011. *Power Electronics*. McGraw-Hill Companies, Inc., New York, NY 10020.

Hua, CC., and Lin, MY. 2000. A Study of Charging Control of Lead-Acid Battery for Electric Vehicles. *IEEE International Symposium on Industrial Electronics*, 1:135-140.

Karami, H., Shamsipur, M., Ghasemi, S., and Mousavi, MF. 2007. Lead-Acid Bipolar Battery Assembled with Pri. Chem Fo. Positive Pasted Electrode. *Journal of Power Sources*, 164(2): 896-904.

Kirchev, A., Delaille, A., Perrin, M., Lemaire, E., and Mattera, F., 2007. Studies of the Pulse Charge of Lead-Acid Batteries for PV Applications. Part II. Impedance of the Positive Plate Revisited+. *Journal of Power Sources*, 170(2): 495-512.

Lee, CS., Lin HC., and Lai, SY. 2013. Development of fast large lead acid battery charging system using multi-state strategy. *International Journal of Computer, Consumer and Control (IJ3C)*, 2(3): 56-65

Tar, B., and Fayed, A. 2016. An Overview of the Fundamentals of Battery Chargers. *IEEE 59th International Midwest Symposium on Circuits and Systems (MWSCAS)*, 16-19 October, Abu Dhabi, UAE, pp. 1-4.

Woo, DG., Choe, GY., Kim, JS., Lee, BK., Hur, J. and Kang, GB. 2011. Comparison of integrated battery chargers for plug-in hybrid electric vehicles: topology and control. In: *Proceedings of the 2011 IEEE International Electric Machines and Drives Conference*, 14-17 May, Niagara Falls, Ontario, Canada., pp. 1294–1299.

Yilmaz, M. and Krein, PT. 2013. Review of Battery Charger Topologies, Charging Power Levels, and Infrastructure for Plug-In Electric Hybrid Vehicles. *IEEE Transactions on Power Electronics*, 28: 2151-2170